ORIGINAL ARTICLE doi: 10.2176/nmc.oa.2014-0436

Neurol Med Chir (Tokyo) 55, 592–598, 2015 Online June 29, 2015

Anatomical Reproducibility of a Head Model Molded by a Three-dimensional Printer

Kosuke KONDO,[1] Masaaki NEMOTO,[1] Hiroyuki MASUDA,[1] Shinichi OKONOGI,[1] Jun NOMOTO,[1] Naoyuki HARADA,[1] Nobuo SUGO,[1] and Chikao MIYAZAKI[2]

[1]*Department of Neurosurgery (Omori), School of Medicine, Toho University, Tokyo;*
[2]*Department of Neurosurgery (Sakura), School of Medicine, Toho University, Sakura, Chiba*

Abstract

We prepared rapid prototyping models of heads with unruptured cerebral aneurysm based on image data of computed tomography angiography (CTA) using a three-dimensional (3D) printer. The objective of this study was to evaluate the anatomical reproducibility and accuracy of these models by comparison with the CTA images on a monitor. The subjects were 22 patients with unruptured cerebral aneurysm who underwent preoperative CTA. Reproducibility of the microsurgical anatomy of skull bone and arteries, the length and thickness of the main arteries, and the size of cerebral aneurysm were compared between the CTA image and rapid prototyping model. The microsurgical anatomy and arteries were favorably reproduced, apart from a few minute regions, in the rapid prototyping models. No significant difference was noted in the measured lengths of the main arteries between the CTA image and rapid prototyping model, but errors were noted in their thickness ($p < 0.001$). A significant difference was also noted in the longitudinal diameter of the cerebral aneurysm ($p < 0.01$). Regarding the CTA image as the gold standard, reproducibility of the microsurgical anatomy of skull bone and main arteries was favorable in the rapid prototyping models prepared using a 3D printer. It was concluded that these models are useful tools for neurosurgical simulation. The thickness of the main arteries and size of cerebral aneurysm should be comprehensively judged including other neuroimaging in consideration of errors.

Key words: three-dimensional printer, rapid prototyping, cerebral aneurysm, computed tomography angiography, microsurgical anatomy

Introduction

Rapid prototyping was invented in the early 1980s,[1,2] and various models started to be used practically with the acceleration of industrialization in the 1990s. A liquid-based process, stereolithography (STL),[1,2] a powder-based process, three-dimensional (3D) printing,[3–5] and a solid-based process, fused deposition modeling,[6] are available. The application of rapid prototyping has recently been rapidly expanding in the field of clinical medicine because of the need for only a short time for preparation and the operability for non-professional engineers.[3–5,7–15] It is frequently used for surgical simulation in the field of surgery.[3–5,7,8,16] Its use is roughly divided into esthetic,[4,5,7] functional,[5,7,8] and educational applications.[3,16] Esthetic application for facial bones and the skull has been reported.[4,5,7] Regarding functional application, it has been used to prepare a tool to adjust the knee joint surface in surgery for gonarthrosis.[8] It has also been reported that occlusal function was improved by the use of a rapid prototyping model for repair of the mandible.[5,7] Regarding educational application, skull base tumor[16] and a whole aorta model[3] were molded and used for surgical education and simulation. An attempt has also been made to prepare rapid prototyping models of injured organs based on postmortem medical images to make them easily understood by court lawyers.[17] In the neurosurgical field in which microsurgery is mainly performed, high-level reproducibility of microsurgical anatomy is required in 3D head models for simulation. However, the level of accuracy of 3D head models prepared by rapid prototyping with regard to reproduction of the original medical image has not yet been clarified. We prepared rapid prototyping models of heads with unruptured cerebral aneurysm based on image

Received December 15, 2014; Accepted April 25, 2015

data of 3D computed tomography angiography (CTA) using a 3D printer. The objective of this study was to evaluate the anatomical reproducibility and accuracy of skull bone and arteries in the rapid prototyping models by comparison with the CTA images on a monitor.

Patient Population

The subjects were 22 patients who underwent CTA of preoperative unruptured cerebral aneurysm between January 2013 and July 2014 at the Department of Neurosurgery, Toho University Omori Medical Center. There were 9 male and 13 female patients aged 43–82 years (mean: 66.2 ± 11.2 years). Cerebral aneurysm was located in the middle cerebral artery (MCA) in nine patients, internal carotid artery (IC) in nine, anterior communicating artery (A-com) in three, and basilar artery (BA) in one.

Methods

I. Preparation of 3D fusion CTA image

The device used was a 64-row × 2 multi-detector CT (SOMATOM Definition Flash, SIEMENS, Munich, Germany). The acquisition conditions were: acquisition interval, 0.4 mm; slice thickness, 0.625 mm; scan speed, 0.5 sec/cycle; and pitch factor, 0.75. A total of 45–60 mL of contrast medium was injected at a rate of 4 mL/sec. CTA image data in digital imaging and communications in medicine (DICOM) data format were transferred online to computer software, namely, an integrated medical image system (SYNAPSE VINCENT: Fuji Film Co., Tokyo). The images of the skull bone and arteries were extracted based on the image thresholds, and the image of the brain stem was extracted by manually setting a region of interest (ROI). A 3D fusion image of the skull bone, arteries, and brain stem was then prepared. Since these images were originally derived from the same data, positional information was common among them. Therefore, there was no need to set the positions in image synthesis. The window width and level of the images were set so as to acquire the most favorable visualization of the skull bone, main arteries, and brain stem in each patient. A portion of the skull bone was removed in the 3D fusion image to observe the interior. The visualization range was from the foramen magnum to the upper margin of the squamous suture in the vertical direction, and from the side with cerebral aneurysm to the opposite anterior clinoid process beyond the midline in the lateral direction. When cerebral aneurysm was present on the midline, the range was judged in each case.

II. Conversion of DICOM to STL data format

To work with a 3D printer, CTA image data in DICOM data format were converted to STL data format using the integrated medical image system. The image setting in DICOM data format, such as the window width and level, was not retained, and it was initialized. After conversion of the data format, images in STL data format were not visualized similarly to those in DICOM data format. Thus, the window width and level of the STL data format images were subjectively reset to make them consistent with the images visualized by DICOM data format.

III. Molding of rapid prototyping model

Three-dimensional image data in STL data format were transferred to a computing system for 3D molding (Freeform: 3D Systems Co., South Calorina, USA) and output to a 3D printer. A 3D printer (Z Printer 450: 3D Systems Co., South Calorina, USA) employing a laminating shaping method, binder jetting, was used. In this method, material powder mainly comprised of plaster (zp®150 powder: 3D Systems Co., South Calorina, USA) was laminated, piled up at 0.1 mm, and molded by solidification with a special glue (zb®63 Clear binder, 3D Systems Co., South Calorina, USA). This approach was fully automatic with full color using an ink-jet system (hp 11: Hewlett Packard Co., California, USA). The resolution of this 3D printer was 300 × 450 dots per inch (dpi), and the minimum feature size was 0.15 mm. Since the vertical build speed of this device was 23 mm/hour, preparation of a rapid prototyping model with a 14–15-cm height took 6–7 hours. The molded rapid prototyping model was buried in white material powder in the device. The model was taken out, and adhering excess material power was removed using an exclusive air spray. An exclusive wax mainly comprised of paraffin was heated to liquid and applied to the model to increase physical strength. When the exclusive wax was excessively applied, it was dissolved using a heat gun (Hakko heating gun 882: Hakko Co., Osaka) and removed.

IV. Evaluation method

1. Microanatomical reproducibility of skull bone

First, visualization of microsurgical anatomy at the following 21 sites of skull bone on CTA was evaluated by a neurosurgeon (S.O.) (Fig. 1A): The spine of Henle, temporal line, external occipital tubercle, jugular tubercle, and arcuate eminence were selected as anatomical bone processus, the vestibular aqueduct, trigeminal impression, groove of greater superficial petrosal nerve (GSPN), lambdoid suture, parieto-mastoid suture, occipito-mastoid

suture, squamous suture, and asterion were selected as recessus, and the superior orbital fissure, foramen rotundum, foramen ovale, foramen lacerum, foramen spinosum, internal auricular canal, jugular foramen, and foramen of mastoid emissary vein were selected as foramens. Reproducibility of the microsurgical anatomy of these sites in the rapid prototyping models prepared by the 3D printer was evaluated by another neurosurgeon (N.S.) (Fig. 1B), and the visualization ability was compared with CTA.

2. Reproducibility of arteries

The following 22 arteries on CTA were selected, and their reproducibility was evaluated by a neurosurgeon (S.O.) (Fig. 1C): the IC, posterior communicating artery (P-com), anterior choroidal artery, anterior cerebral artery (A1, A2, A3, A4), medial striate artery (MSA), MCA [M1, M2 (superior portion, inferior portion), M3, M4], lateral striate artery (LSA), BA, vertebral artery (VA), posterior cerebral artery (P1, P2, P3), superior cerebellar artery (SCA), anterior inferior cerebellar artery (AICA), and posterior inferior cerebellar artery (PICA).[18–20] Reproducibility of these arteries in the rapid prototyping models was evaluated by another neurosurgeon (N.S.) (Fig. 1D) and the visualization ability was compared with CTA.

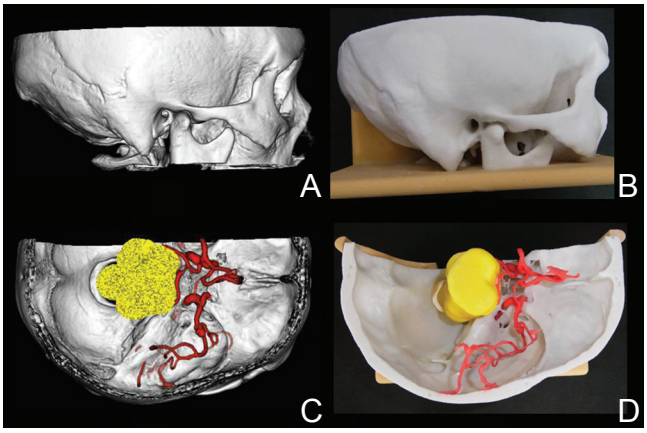

Fig. 1 CTA and rapid prototyping model. A: Lateral view of CTA, B: lateral view of rapid prototyping model, C: upper view of CTA, and D: upper view of rapid prototyping model. CTA: computed tomography angiography.

3. Measurement of length and thickness of the main arteries and size of cerebral aneurysm

The lengths of A1 and M1, thickness of IC, A1, and M1, and size of cerebral aneurysm on CTA were measured on a monitor using software attached to the integrated medical image system (S.O.). The arterial length was measured setting the baseline to the intersection point of the axes of the arteries, not based on the outer wall: For the length of A1, the linear distance from the intersection point of A1, M1, and IC axes to the intersection point of A-com, A1, and A2 axes was measured. For the length of M1, the linear distance from the intersection point of A1, M1, and IC axes to the intersection point of M1 and M2 (superior portion and inferior portion) axes was measured (Fig. 2A). The thickness of IC, A1, and M1 was measured at the site closest to the carotid bifurcation (Fig. 2B). In terms of the size of cerebral aneurysm, the maximum transverse and longitudinal diameters and the maximum diameter of the aneurysmal neck were measured (Fig. 2C). These were also measured based on the same baselines in the rapid prototyping model prepared by the 3D printer (N.S.) (Fig. 2D–F) using a drawing instrument, a type of compass with needle tips on both legs, Dividers [83A-4 "Yankee" Spring-Type Dividers (150 mm): the L.S. Starrett Co., Massachusetts, USA]. The needle points of the legs of Dividers were set to the region between the target points, and the distance was measured using a digital caliper [Shinwa Rules digital caliper model 19975: Shinwa Rules Co., Tsubame, Niigata]. The measured values of the same anatomical regions

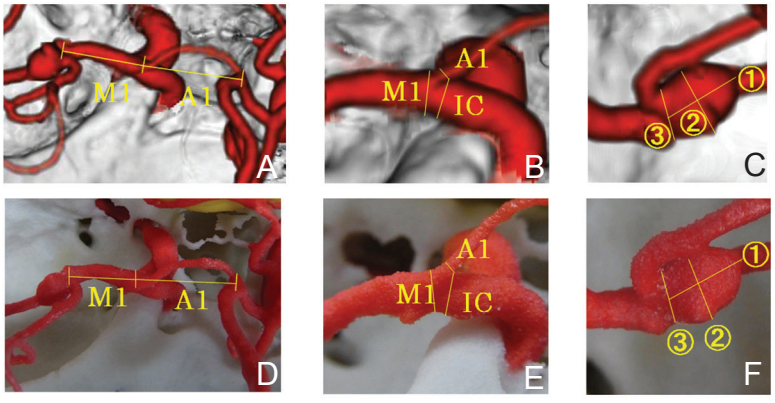

Fig. 2 Arteries on CTA and rapid prototyping model. A: Measurement regions in the length of A1 and M1 on CTA , B: measurement regions in the width of A1, M1, and IC on CTA, C: measurement regions in the aneurysmal sizes on CTA, D: measurement regions in the length of A1 and M1 on rapid prototyping model, E: measurement regions in the width of A1, M1, and IC on rapid prototyping model, F: measurement regions in the aneurysmal sizes on rapid prototyping model, ①: longitudinal diameter of aneurysm, ②: transverse diameter of aneurysm, ③: diameter of aneurysmal neck, CTA: computed tomography angiography.

were compared between the CTA image and the rapid prototyping model.

In statistical analysis, reproducibility of the skull bone and arteries in the rapid prototyping models was analyzed using the McNemar test. For comparison of the arterial length and thickness and size of cerebral aneurysm, the paired t-test was used. $P < 0.05$ was regarded as significant (IBM SPSS Statistics, ver. 19, IBM Co., New York, USA). This study was approved by the Ethics Committee of Toho University Omori Medical Center (approval number: 26-129).

Results

I. Reproducibility of skull bone in rapid prototyping model

Overall reproducibility of microsurgical anatomy in the rapid prototyping models was favorable (Table 1). The reproducibility levels of the GSPN ($p < 0.01$), foramen spinosum ($p < 0.01$), and foramen of the mastoid emissary vein ($p < 0.001$) were significantly low.

II. Reproducibility of arteries in rapid prototyping model

The reproducibility levels of the IC, A1, A2, A3, M1, M2 (superior and inferior branch), BA, P1, and P3 relative to visualization on CTA were 95% or greater (Table 2). In contrast, the reproducibility levels of LSA and AICA were significantly lower ($p < 0.05$).

III. Comparison of measured values of the main arteries and cerebral aneurysm

No significant difference was noted in the measured length of A1 or M1 between the CTA image and rapid prototyping model (Table 3). In contrast, the thickness of IC, A1, and M1 was significantly greater in the rapid prototyping model than in the CTA image, showing errors ($p < 0.001$). The longitudinal diameter of cerebral aneurysm was also greater in the rapid prototyping model ($p < 0.01$).

Table 1 Reproducibility of skull bone in rapid prototyping model

Microanatomical region	CTA n (%)	RP model n (%)	RP model /3DCTA (%)
Processus			
external occipital tubercle	22 (100)	22 (100)	(100)
arcuate eminence	22 (100)	22 (100)	(100)
jugular tubercle	22 (100)	19 (86.4)	(86.4)
spine of Henle	22 (100)	17 (77.3)	(77.3)
temporal line	17 (77.3)	17 (77.3)	(100)
Recessus			
trigeminal impression	22 (100)	22 (100)	(100)
vestibular aqueduct	22 (100)	20 (90.9)	(90.9)
GSPN	22 (100)	14 (63.6)	(63.6) **
lambdoid suture	21 (95.5)	21 (95.5)	(100)
Asterin	19 (86.4)	19 (86.4)	(100)
occipito-mastoid suture	18 (81.8)	18 (81.8)	(100)
squamous suture	18 (81.8)	18 (81.8)	(100)
parieto-mastoid suture	17 (77.3)	17 (77.3)	(100)
Foramen			
internal auricular canal	22 (100)	22 (100)	(100)
jugular foramen	22 (100)	22 (100)	(100)
superior orbital fissure	22 (100)	21 (95.5)	(95.5)
foramen lacerum	22 (100)	21 (95.5)	(95.5)
foramen ovale	22 (100)	20 (90.9)	(90.9)
foramen rotundum	22 (100)	19 (86.4)	(86.4)
foramen spinosum	22 (100)	13 (59.1)	(59.1)**
foramen of mastoid emissary vein	17 (77.3)	2 (9.1)	(11.8)***

3DCTA: three-dimensional computed tomography angiography, GSPN: groove of greater superficial petrosal nerve, RP model: rapid prototyping model, **: $p < 0.01$, ***: $p < 0.001$.

Discussion

Several studies on the accuracy of rapid prototyping models of dry human skull have been performed.[21–23] In a study comparing the linear distances between several anatomical landmarks between the rapid prototyping model and dry human skull, errors were very small (0.62 ± 0.35 mm),[21] showing a high accuracy level. In clinical cases, since it is impossible to measure anatomical landmarks in the body of patients directly, rapid prototyping models are compared with medical images. Accordingly, it is necessary to identify the level of reproduction of the original medical image in the rapid prototyping model from a practical clinical viewpoint.

3DCTA data of the unruptured cerebral aneurysms were selected to evaluate the anatomical reproducibility of a head model molded by a 3D printer, for the following reasons: multiple anatomical regions can be readily measured because bone, normal arteries, and a cerebral aneurysm are simultaneously visualized in 3DCTA data, positioning of the arteries and bone in image preparation is unnecessary, and

Table 2 Reproducibility of arteries in rapid prototyping model

Arteries	CTA n (%)	RP model n (%)	RP model /3DCTA (%)
IC	22 (100)	22 (100)	(100)
P-com	9 (40.9)	8 (36.4)	(88.9)
Ant ch	0 (0.0)	0 (0.0)	(–)
A1	21 (95.5)	20 (90.9)	(95.2)
A2	22 (100)	21 (95.5)	(95.5)
A3	10 (45.5)	10 (45.5)	(100)
A4	2 (9.1)	0 (0.0)	(0.0)
MSA	2 (9.1)	1 (4.5)	(50.0)
M1	22 (100)	22 (100)	(100)
M2 sup	22 (100)	22 (100)	(100)
M2 inf	22 (100)	22 (100)	(100)
M3	17 (77.3)	12 (54.5)	(70.6)
M4	1 (4.5)	0 (0.0)	(0.0)
LSA	9 (40.9)	2 (9.1)	(22.2)*
BA	22 (100)	21 (95.5)	(95.5)
VA	22 (100)	17 (77.3)	(77.3)
P1	20 (90.9)	19 (86.4)	(95.0)
P2	22 (100)	20 (90.9)	(90.9)
P3	11 (50.0)	11 (50.0)	(100)
SCA	19 (86.4)	17 (77.3)	(89.5)
AICA	10 (45.5)	3 (13.6)	(30.0)*
PICA	16 (72.7)	12 (54.5)	(75.0)

A1: this segment originates from the internal carotid artery and extends to the anterior communicating artery, A2: this segment extends from the anterior communicating artery to the bifurcation forming the pericallosal and callosomarginal arteries, A3: this segment extends around the genu of the corpus callosum, A4: this segment is located above the corpus callosum, AICA: anterior inferior cerebellar artery, Ant ch: anterior choroidal artery, BA: basilar artery, CTA: computed tomography angiography, IC: intracranial internal carotid artery, LSA: lenticulo-striate artery, M1: the course of this segment is in the sphenoidal compartment, M2 inf: inferior division of M2, M2 sup: superior division of M2, M3: this segment passes over the surface of the opercula, M4: this segment courses on the cortical surface, MSA: medial striate artery, P1: this segment extends from the tip of the basilar artery to the origin of the posterior communicating artery, P2: this segment extends from the posterior communicating artery to the dorsal aspect of the midbrain, P3: this segment extends from the lateral aspect of the quadrigeminal cistern at the origin of the posterior temporal artery, P-com: posterior communicating artery, PICA: posterior inferior cerebellar artery, RP model: rapid prototyping model, SCA: superior cerebellar artery, VA: vertebral artery, *: $p < 0.05$.

Table 3 Measured values in arteries and cerebral aneurysms

	CTA (mm)	RP model (mm)
Arteries		
length of A1	16.3 ± 2.3	15.8 ± 1.6
length of M1	19.9 ± 5.1	18.8 ± 5.6
width of IC	3.4 ± 0.8	4.2 ± 0.6***
width of A1	2.1 ± 0.7	2.7 ± 0.6***
width of M1	2.9 ± 0.6	3.5 ± 0.5***
Aneurysm		
width of neck	4.7 ± 2.8	5.3 ± 3.0
transverse	6.9 ± 6.0	7.5 ± 6.7
longitudinal	6.7 ± 6.8	7.7 ± 6.9**

A1: A1 segment of anterior cerebral artery, CTA: computed tomography angiography, IC: intracranial internal carotid artery, M1: M1 segment of middle cerebral artery, RP model: rapid prototyping model, **: $p < 0.01$, ***: $p < 0.001$.

3DCTA is frequently needed to clinically diagnose an unruptured cerebral aneurysm.

Factors influencing the accuracy and reproducibility of rapid prototyping models prepared based on CTA are roughly divided into image processing and model manufacturing.[6,24,25] Problems with the first factor, image processing, may be produced mainly by conversion of DICOM to STL data format.[24] STL data format[2,26] is a system expressing 3D shapes as collections of small triangles. This is used as the standard format in the rapid prototyping field because the data structure is simple. However, STL data format is basically incapable of expressing elements other than planes, such as dots and lines, and continuity of colors and planes. Thus, when images visualized in DICOM data format are converted to STL data format, fine shapes are likely to be destroyed or lost due to reduction of smoothing and the number of planes. Generally, many devices of image display are added to computer software for analysis of 3D images to present DICOM data format images clearly, such as window width and level, image threshold, transparency, edge enhancement and smoothing, and gamma correction. However, these settings of display are initialized by conversion to STL data format, and the converted image is visually different from the original image in DICOM data format. To prepare a rapid prototyping model close to the actual CTA image, subjective resetting of the window width and level in STL data format images is inevitable. Differences in measured values between the CTA image and rapid prototyping model were noted in the thickness of the main arteries and size of the cerebral aneurysm, which may have been due to image data errors produced by conversion of DICOM to STL data format and the influence of resetting the window width and level on molding of the external vascular walls. The reason for the greater measured thickness in the rapid prototyping model may have been a bias added to secure physical

vulnerability of the rapid prototyping model by the person who prepared it. Moreover, an error of the major axis of the cerebral aneurysm was noted in the rapid prototyping model. The size of unruptured cerebral aneurysm is a risk factor of rupture, and evaluation on the order of mm is necessary.[27] The size of unruptured cerebral aneurysm should be comprehensively judged based on not only the rapid prototyping model but also values measured in other neuroimages including CTA. The lengths of the main arteries were not different between the CTA image and the rapid prototyping model, showing high-level accuracy of the reproduction. This may have been due to setting the baseline to the center of the blood vessels, which may have reduced errors produced by conversion to STL data format. To increase the accuracy of molding of rapid prototyping models, development of a method to reduce image data errors produced by conversion of data format is desired.

The second factor influencing the reproducibility and accuracy of rapid prototyping models is breakage of fine parts accompanying model manufacturing.[23] Among many processes of this method, those likely to break the rapid prototyping model include taking out the model buried in white material powder in the device, removal of excessive material powder adhering to the model using an air spray, application of the exclusive wax heated to liquid to the model, and removal of excessively applied exclusive wax by reheating it using a heat gun. We investigated the reproducibility of the arteries to evaluate physical vulnerability associated with model manufacturing. It was demonstrated that thick arteries, IC, A1, A2, A3, M1, M2, BA, P1, and P3, are stably molded. In contrast, the reproducibility of thin arteries, LSA and AICA, was poor. These findings reflected breakage of fine parts by model manufacturing, suggesting a limit of physical strength of rapid prototyping models prepared using this device. The relationship between the length and thickness is involved in the physical strength of a molded long object, such as blood vessels. BA and VA and their branches passing a long distance in the region anterior to the brain stem are important blood vessels and anatomically essential for surgical simulation. To reduce breakage of these arteries, the brain stem present near these vessels was simultaneously molded to support them. Consideration of the physical strength of vulnerable regions may be necessary when a rapid prototyping model is prepared. Overall anatomical reproducibility of skull bone was favorable, but reproducibility of small foramens and shallow grooves, such as the GSPN, foramen spinosum, and foramen of the mastoid emissary vein, was poor. This may have been due to the influences of the image processing and manufacturing process, such as resetting of the window width and level, insufficient removal of material powder, and thick application of wax.

The preparation of a high-precision rapid prototyping model in millimeter units may lead to the development of a simulation system for microsurgery comparable to cadaver dissection in the future. For diseases with surgical difficulty, such as skull base tumors, improvement of the accuracy of surgical simulation is expected to improve not only operator education but also the surgical success rate. Simplification of the rapid prototyping model preparation method using a 3D printer will reduce the device and material costs, which may lead to its wide application in clinical medicine.

Conclusion

Regarding the CTA image as the gold standard, in rapid prototyping models prepared using a 3D printer, the microsurgical anatomy of skull bone and main arteries was favorably reproduced, and the vascular lengths were also molded with high-level accuracy. It was concluded that rapid prototyping models prepared by this procedure are useful for neurosurgical simulation. On the other hand, the thickness of arteries and size of cerebral aneurysm may be erroneous. These should be comprehensively judged including other neuroimaging.

Acknowledgment

The authors thank and appreciate Chiaki Nishimura, Professor Emeritus of Toho University for helping them with the statistical processing. They also appreciate Kazuhiro Tachiki at Toho University Medical Center for molding of the rapid prototyping models in this study.

Conflicts of Interest Disclosure

The authors have no personal, financial, or institutional interest in any of the drugs, materials, or devices in the article. All authors who are members of The Japan Neurosurgical Society (JNS) have registered online Self-reported COI Disclosure Statement Forms through the website for JNS members.

References

1) Kodama H: Automatic method for fabricating a three-dimensional plastic model with photo-hardening polymer. *Rev Sci Instrum* 52: 1770–1773, 1981
2) Hull C: Washington, DC: US Patent Office; 4,575,330; Apparatus for production of three-dimensional

objects by stereolithography [Internet]. Available from: http://www.google.com/patents/US4575330.
3) Håkansson A, Rantatalo M, Hansen T, Wanhainen A: Patient specific biomodel of the whole aorta—the importance of calcified plaque removal. *VASA* 40: 453–459, 2011
4) Kim BJ, Hong KS, Park KJ, Park DH, Chung YG, Kang SH: Customized cranioplasty implants using three-dimensional printers and polymethylmethacrylate casting. *J Korean Neurosurg Soc* 52: 541–546, 2012
5) Saijo H, Kanno Y, Mori Y, Suzuki S, Ohkubo K, Chikazu D, Yonehara Y, Chung UI, Takato T: A novel method for designing and fabricating custom-made artificial bones. *Int J Oral Maxillofac Surg* 40: 955–960, 2011
6) Ibrahim D, Broilo TL, Heitz C, de Oliveira MG, de Oliveira HW, Nobre SM, Dos Santos Filho JH, Silva DN: Dimensional error of selective laser sintering, three-dimensional printing and PolyJet models in the reproduction of mandibular anatomy. *J Craniomaxillofac Surg* 37: 167–173, 2009
7) Li J, Hsu Y, Luo E, Khadka A, Hu J: Computer-aided design and manufacturing and rapid prototyped nanoscale hydroxyapatite/polyamide (n-HA/PA) construction for condylar defect caused by mandibular angle ostectomy. *Aesthetic Plast Surg* 35: 636–640, 2011
8) Kunz M, Waldman SD, Rudan JF, Bardana DD, Stewart AJ: Computer-assisted mosaic arthroplasty using patient-specific instrument guides. *Knee Surg Sports Traumatol Arthrosc* 20: 857–861, 2012
9) Niikura T, Sugimoto M, Lee SY, Sakai Y, Nishida K, Kuroda R, Kurosaka M: Tactile surgical navigation system for complex acetabular fracture surgery. *Orthopedics* 37: 237–242, 2014
10) Waran V, Narayanan V, Karuppiah R, Pancharatnam D, Chandran H, Raman R, Rahman ZA, Owen SL, Aziz TZ: Injecting realism in surgical training-initial simulation experience with custom 3D models. *J Surg Educ* 71: 193–197, 2014
11) Rankin TM, Giovinco NA, Cucher DJ, Watts G, Hurwitz B, Armstrong DG: Three-dimensional printing surgical instruments: are we there yet? *J Surg Res* 189: 193–197, 2014
12) Lueders C, Jastram B, Hetzer R, Schwandt H: Rapid manufacturing techniques for the tissue engineering of human heart valves. *Eur J Cardiothorac Surg* 46: 593–601, 2014
13) Chae MP, Hunter-Smith DJ, Spychal RT, Rozen WM: 3D volumetric analysis for planning breast reconstructive surgery. *Breast Cancer Res Treat* 146: 457–460, 2014
14) Harada N, Kondo K, Miyazaki C, Nomoto J, Kitajima S, Nemoto M, Uekusa H, Harada M, Sugo N: Modified three-dimensional brain model for study of the trans-sylvian approach. *Neurol Med Chir* (*Tokyo*) 51: 567–571, 2011
15) Mori K, Yamamoto T, Nakao Y, Esaki T: Development of artificial cranial base model with soft tissues for practical education: technical note. *Neurosurgery* 66: 339–341; discussion 341, 2010
16) Oishi M, Fukuda M, Yajima N, Yoshida K, Takahashi M, Hiraishi T, Takao T, Saito A, Fujii Y: Interactive presurgical simulation applying advanced 3D imaging and modeling techniques for skull base and deep tumors. *J Neurosurg* 119: 94–105, 2013
17) Ebert LC, Thali MJ, Ross S: Getting in touch—3D printing in forensic imaging. *Forensic Sci Int* 211: e1–e6, 2011
18) Perlmutter D, Rhoton AL: Microsurgical anatomy of the distal anterior cerebral artery. *J Neurosurg* 49: 204–228, 1978
19) Gibo H, Carver CC, Rhoton AL, Lenkey C, Mitchell RJ: Microsurgical anatomy of the middle cerebral artery. *J Neurosurg* 54: 151–169, 1981
20) Yasargil MG: *Microneurosurgery*. Stuttgart, George Thieme Verlag, vol 2, 1984, pp 260–269
21) Choi JY, Choi JH, Kim NK, Kim Y, Lee JK, Kim MK, Lee JH, Kim MJ: Analysis of errors in medical rapid prototyping models. *Int J Oral Maxillofac Surg* 31: 23–32, 2002
22) Taft RM, Kondor S, Grant GT: Accuracy of rapid prototype models for head and neck reconstruction. *J Prosthet Dent* 106: 399–408, 2011
23) Silva DN, Gerhardt de Oliveira M, Meurer E, Meurer MI, Lopes da Silva JV, Santa-Bárbara A: Dimensional error in selective laser sintering and 3D-printing of models for craniomaxillary anatomy reconstruction. *J Craniomaxillofac Surg* 36: 443–449, 2008
24) Huotilainen E, Jaanimets R, Valášek J, Marcián P, Salmi M, Tuomi J, Mäkitie A, Wolff J: Inaccuracies in additive manufactured medical skull models caused by the DICOM to STL conversion process. *J Craniomaxillofac Surg* 42: e259–e265, 2014
25) Hirsch DL, Garfein ES, Christensen AM, Weimer KA, Saddeh PB, Levine JP: Use of computer-aided design and computer-aided manufacturing to produce orthognathically ideal surgical outcomes: a paradigm shift in head and neck reconstruction. *J Oral Maxillofac Surg* 67: 2115–2122, 2009
26) Mankovich NJ, Cheeseman AM, Stoker NG: The display of three-dimensional anatomy with stereolithographic models. *J Digit Imaging* 3: 200–203, 1990
27) UCAS Japan Investigators; Morita A, Kirino T, Hashi K, Aoki N, Fukuhara S, Hashimoto N, Nakayama T, Sakai M, Teramoto A, Tominari S, Yoshimoto T: The natural course of unruptured cerebral aneurysms in a Japanese cohort. *N Engl J Med* 366: 2474–282, 2012

Address reprint requests to: Nobuo Sugo, MD, PhD, Department of Neurosurgery (Omori), School of Medicine, Faculty of Medicine, Toho University, 6-11-1 Omori-nishi, Ota-ku, Tokyo 143-8541, Japan. *e-mail*: nsugo@med.toho-u.ac.jp